Electric field gradient in ferromagnetic iron measured with beta-detected modulated adiabatic passage on oriented nuclei

W. D. Hutchison,[1] D. H. Chaplin,[1] S. Ohya,[2] S. Muto,[3] K. Nishimura,[4] H. Sato,[2] Y. Kawamura,[2] and A. E. Stuchbery[5]
[1]*School of Physics, University College, The University of New South Wales, Australian Defence Force Academy, Canberra ACT 2600, Australia*
[2]*Department of Physics, Niigata University, Niigata 950-2181, Japan*
[3]*National Laboratory for High Energy Physics, Tsukuba 350, Japan*
[4]*Faculty of Engineering, Toyama University, Toyama 930-8555, Japan*
[5]*Department of Nuclear Physics, Research School of Physical Sciences and Engineering, The Australian National University, Canberra ACT 0200, Australia*
(Received 10 July 2002; published 30 October 2002)

Modulated adiabatic passage on oriented nuclei has been used in combination with beta-ray detection to make a definitive measurement of a nuclear electric quadrupole hyperfine interaction in elemental iron. For ^{59}Fe in single-crystal iron magnetized along the easy $\langle 100\rangle$ direction $P/h=3eQV_{ZZ}/4I(2I-1)h = +19.4(5)$ kHz, and along the hard $\langle 111\rangle$ direction $P/h=+20.2(5)$ kHz. Theoretical estimates for the ^{59}Fe ground-state nuclear electric quadrupole moment are considered in terms of the particle-rotor model and the shell model. A value of $Q=+0.19(3)$ b is adopted, which, in turn, is used to obtain electric field gradient values at the Fe site of $V_{ZZ}=+1.7(3)\times10^{19}$ V m^{-2} and $+1.8(3)\times10^{19}$ V m^{-2} for magnetization along the easy and hard directions, respectively. Comparisons are made with previously measured results for the nearby $3d$ impurities Mn and Co in Fe.

DOI: 10.1103/PhysRevB.66.134425 PACS number(s): 76.80.+y, 76.60.−k, 75.50.Bb, 21.10.Ky

I. INTRODUCTION

When a quadrupolar probe nucleus ($I\geqslant 1$) is located substitutionally in a ferromagnetic metal matrix, it will, in general, experience a magnetic dipole hyperfine interaction ($M1$) to first order and an electric quadrupole hyperfine interaction ($E2$) to second order. Typical strengths of $M1$ interactions (excluding non-S state lanthanide probes) are in the range 10–1000 MHz, corresponding to the presence of static, internal magnetic hyperfine fields of a few tesla up to a few hundred tesla. Over the past three decades, considerable effort has been placed on measuring the relatively large $M1$ interactions, and hence magnetic hyperfine fields for those probes with known nuclear magnetic dipole moments.[1,2] This in turn has led to significant progress in *ab initio* band-structure calculations, endeavoring to reproduce these magnetic hyperfine fields[3–5] and, more recently, nuclear-spin-lattice relaxation rates,[4,6] especially with ferromagnetic Fe as the host.

In contrast, there have been very few attempts to calculate the corresponding solid-state contribution to $E2$, the electric field gradient (efg) in magnetically ordered metals, apart from initial activity immediately following the discovery of the nonzero efg in crystallographically cubic Fe and Ni during the early 1970s.[7–9] This lack of theoretical followup presumably reflects the initial difficulty in obtaining reliable experimental data since the strengths of the intrinsic $E2$ interactions are typically only a few tens to a few hundred kHz. Concerns were raised regarding potential competition from extrinsic factors such as strain in polycrystalline hosts[10] and excessive impurity concentration, as required in conventional NMR to compensate sensitivity limitations. Only for a very select few, low spin, heavy ($5d$) probes (e.g., ^{191,193}Ir) in Fe or Ni where the $E2$ interaction is readily resolvable, has it been measured in the conventional NMR frequency domain. For lighter probes (e.g., $3d$, $4d$) the $E2$ splitting is easily swamped by magnetic inhomogeneous broadening from distributions in demagnetizing fields, which are maximized in nonspheroidal ferromagnets. In addition, and especially in the 1970s, the quantity and quality of nuclear electric quadrupole moments did not (and does not), match the accumulated data set for nuclear magnetic dipole moments.

In the interim, improvements in experimental technique, especially modulated adiabatic passage on oriented nuclei (MAPON),[11] and the realization of the importance of nuclear deformation in nuclear structure modeling, leading to marked improvements in the nuclear quadrupole moment data set, implies the field is poised to be developed in a similar fashion to that of magnetic hyperfine fields. It is the purpose of this paper to provide efg systematics for $3d$ impurities in single-crystal ferromagnetic iron by extending MAPON spectroscopy to beta detection to enable the important pure Fe case to be studied, a circumstance which is a lockout in conventional NMR, technically inhibitive for gamma-detected nuclear magnetic resonance on oriented nuclei (NMRON), and arguably at the limit of the capabilities of Mössbauer effect spectroscopy (MES). It should be noted that an early attempt to measure an electric quadrupole interaction (EQI) in iron was indeed via MES.[12] However, not only was the precision of the result poor but also this work utilized rolled thin polycrystalline foils and was subsequently largely discredited by others[10] on the grounds that the EQI's obtained were thought to be dominated by strain in the specimens. These later authors attempted MES measurements of iron, via ^{57}Fe plated single crystals, finding an apparent increase in the EQI from the $\langle 100\rangle$ to the $\langle 111\rangle$ directions.

However, the results could not be reproduced and it was again concluded that strain and imperfection appeared to be dominant. With the benefit of the superior resolution of MAPON, it is now well established that high quality, carefully prepared single crystals, well annealed after the introduction of the probes, are best used for measurement of intrinsic EQI's in nominally cubic hosts. In the case of pure iron, the present MAPON results allow comparison with the pioneering MES work and this is done in the discussion.

Comparisons are also made in the discussion with MAPON results from other ferromagnetic hosts. It is hoped that this data set will stimulate a re-emergence of theoretical activity in the field, especially as the efg for the $3d$ impurities will reflect to a large extent the inability of crystal fields to completely quench the orbital angular momentum of the impurity probes own atomic electrons, whereas S state impurity ions, e.g., Mn^{2+}, will provide direct information on intraionic shielding effects and/or conduction electron contributions to the efg. One striking advantage of these systematics in crystallographically cubic ferromagnets, relative to magnetic hyperfine field calculations, is the lack of complication from a substantial host contribution.

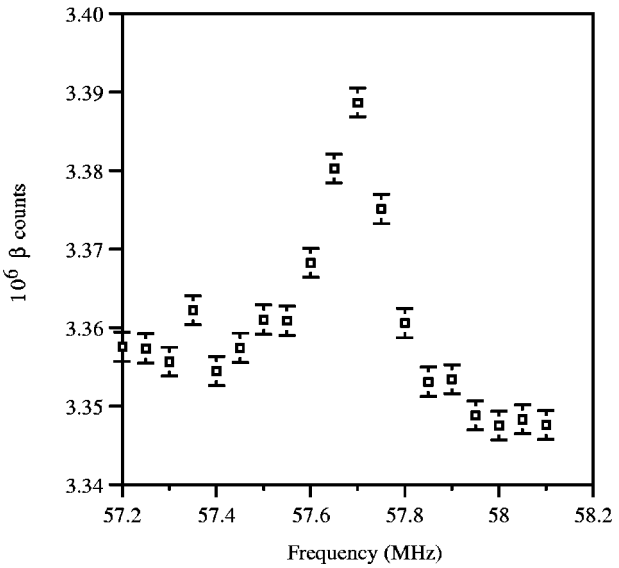

FIG. 1. Beta-detected CW NMRON of a ^{59}FeFe single crystal with 0.2 T applied along ⟨100⟩. The FM amplitude was ±50 kHz and the modulation frequency was 100 Hz.

II. EXPERIMENTAL DETAILS

Iron single-crystal discs of 1 mm thickness, (110) plane, were spark cut to 4 mm diameter and one surface was then mechanically polished using decreasing grain size alumina, down to 0.05 μm. The planar cut and the orientation of the ⟨100⟩ and ⟨111⟩ directions within the plane were confirmed using Laue x-ray back reflection. A drop of HCl solution containing ^{59}Fe activity was placed in the center of the polished surface of each crystal and evaporated to dryness. Crystals were then annealed under an atmosphere of flowing hydrogen gas up to 850 °C for 5 min. A Fick's law calculation, taking into account the finite-temperature rise and fall rates of the furnace and using tabulated values of diffusion coefficients for ^{55}Fe into Fe[13] suggested a root-mean-square diffusion depth of 1.0 μm for these conditions. The active surface was subsequently wiped with ethanol to remove any undiffused activity. Average ^{59}Fe activity remaining on each crystal at this stage was approximately 20 μCi. One of these crystals was soldered to the cold finger of a dilution refrigerator such that a magnetic field could be applied in the plane of the disc and parallel to the particular crystal axis of interest, either the easy ⟨100⟩ or hard ⟨111⟩ direction. An applied field, of 0.2–0.3 T, sufficient to magnetically align the disc was used during the measurements. (Previous MAPON studies of, mostly, Co and Mn probes in single-crystal Fe and Ni hosts have shown no appreciable field dependence of EQI's.[14]) Nearby radio frequency (rf) coils allowed rf fields to be applied in the direction perpendicular to the dc magnetic field and parallel to the crystal surface. For beta-ray detection two 50-mm^2 Si detectors positioned close to 0° and 180° were used. These detectors were mounted on a heat shield, maintained at around 0.7 K, inside the dilution refrigerator and were approximately 8 mm from the center of the sample. Stainless-steel coaxial cables of about 1.2-m length made the connection to the preamplifiers placed outside the cryostat. This configuration, at Niigata University, has been described previously in detail.[15] The cold finger temperature was monitored during the experiment with a ^{60}CoCo nuclear orientation thermometer via gamma-ray detected nuclear orientation and HP Ge detectors placed outside the cryostat. The base temperature, without rf heating, was ~9 mK.

The rf and control electronics used for the adiabatic fast (or single) passage (AFP) and MAPON measurements was similar to the setup in Canberra.[16,17] A linear ramp voltage was applied to the modulation input of the rf generator to create the frequency sweep and a double balance mixer was used to produce the double sideband carrier suppressed rf spectrum for MAPON. Carrier and second sideband suppression was monitored on a spectrum analyzer and was always greater than 40 dB.

III. RESULTS

An example of beta-detected continuous wave (CW) NMRON for the ^{59}FeFe single crystal in an applied field of 0.2 T is shown in Fig. 1. The center frequency is 57.695(6) MHz which is just slightly lower than, and therefore consistent with, the projected zero-field value deduced from earlier Fe foil measurements.[15] The linewidth at full width at half maximum (FWHM) of 162(7) kHz (Lorentzian fit) is somewhat broader than the 97(7) kHz observed in 0.2 T for the foil.[18] The broader single-crystal resonance is predominately due to a larger frequency modulation (FM) amplitude of ±50 kHz versus ±20 kHz used for the foil. However, both a larger spread of bulk demagnetizing fields across the active region of the relatively small 4 mm diameter crystal surface compared to the thin foil as well as the possibility that the average EQI in the foil is smaller and less unique can also not be discounted. In any event, the quadrupolar contribution to the linewidth of the ^{59}FeFe resonances in both these experiments leads to overall linewidths considerably

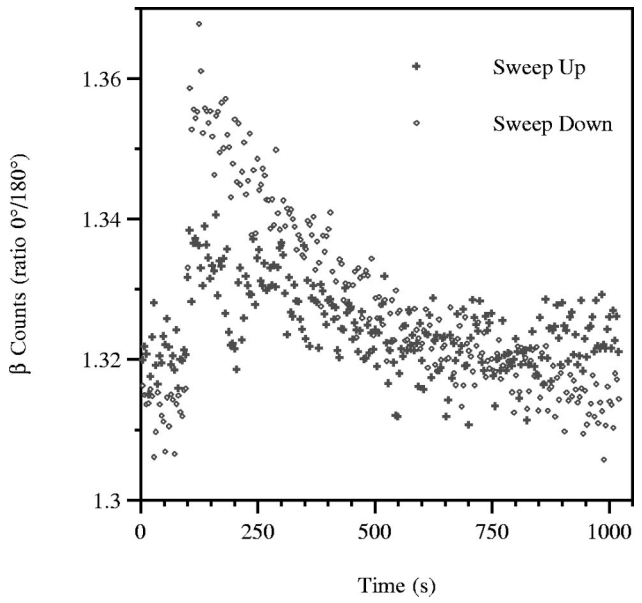

FIG. 2. Beta-detected adiabatic fast passage on a ^{59}FeFe single crystal with 0.2 T applied along ⟨100⟩. The ordinate is the ratio of counts from the 0° and 180° beta detectors. The sweep duration was 0.5 s, covering a 300-kHz range centered at 57.69 MHz.

greater than that found for NMR of naturally abundant spin-1/2 ^{57}FeFe of ~30 kHz.[19]

AFP was performed next as a precursor to MAPON, to optimize sweep and data collection parameters as well as determining the sign of the EQI. Post passage signals for the case with the applied field along the ⟨100⟩ direction are shown in Fig. 2. From this figure it is concluded that the ^{59}FeFe EQI is positive. This conclusion is based on the different post passage responses for the opposite sweep directions.[20] (See AFP sections in Refs. 11 or 16 for further explanation.) The EQI was also found to be positive for the case of the applied magnetic field along the hard ⟨111⟩ direction. As a result of these sign determinations MAPON spectroscopy was performed using sweep down experiments only. The change in beta counts as a function of modulation frequency F_m (MAPON integral data) is shown in Figs. 3(a) and 4(a) for the ⟨100⟩ and ⟨111⟩ directions, respectively. A similar post-passage change was observed for both of the beta detectors in the ⟨100⟩ case with the fractional change of both incorporated in Fig. 3(a). Figure 4(a) is derived from 0° signals only. Figures 3(b) and 4(b) are the differentials obtained from the integral data via a least-squares polynomial fit at each point, considering five (four) points on either side, followed by analytical differentiation. The peak values of the EQI are $P/h=+19.4(5)$ kHz $[+20.2(5)$ kHz$]$ and the FWHM's of the distributions are $\Delta P/h=19(3)$ kHz $[9.9(5)$ kHz$]$ for the ⟨100⟩ (⟨111⟩) directions respectively. Note that the ⟨100⟩ EQI distribution is around twice as broad as that along ⟨111⟩. A similar effect has also been observed from MAPON measurements on $5d$ probes in iron.[21]

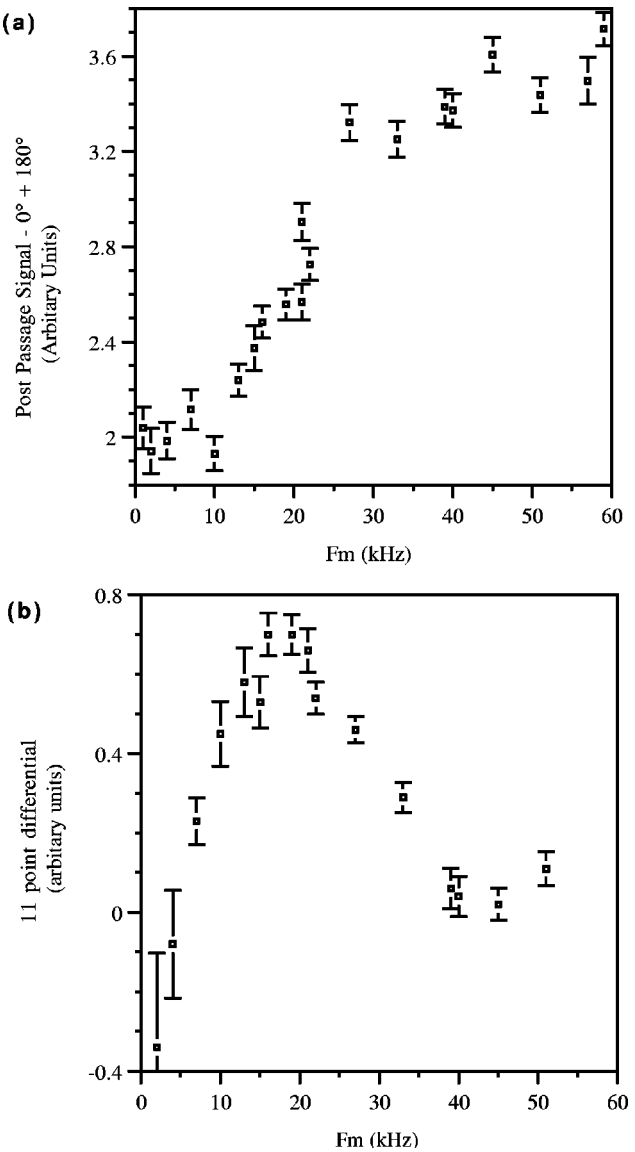

FIG. 3. Beta-detected MAPON on the ^{59}FeFe single crystal with 0.2 T applied along ⟨100⟩. (a) Shows the post passage change in anisotropy for sweep down experiments of 0.5-s duration, covering a 300-kHz range centered at 57.69 MHz. (b) The differential of (a) providing a mode value of $P/h=+19.4(5)$ kHz.

IV. NUCLEAR QUADRUPOLE MOMENT

There has been no experimental determination of the quadrupole moment of the ground state of ^{59}Fe, and the only theoretical value of $Q(^{59}\text{Fe},3/2_1^-)$ in the literature is a rather old estimate based on the Nilsson model.[22] The magnetic moment of the ground state has been measured precisely,[15] but no other experimental static moments or transition rates are available for the low-lying negative parity states.

Recently, the quadrupole moment of the corresponding $3/2^-$ state in ^{57}Fe has been considered in some detail from the point of view of both large-basis nuclear shell-model calculations and solid-state calculations of the electric field gradients required to interpret Mössbauer data.[23] Both the nuclear and solid-state theory lead to a recommended value of $Q(3/2_1^-)=+0.15(2)$, which also agrees with the value $Q(3/2_1^-)=+0.16(1)$ obtained by Dufek *et al.*[24] In due course, these developments should make it possible to obtain a consistent experimental value of $Q(3/2_1^-)$ in ^{59}Fe, but

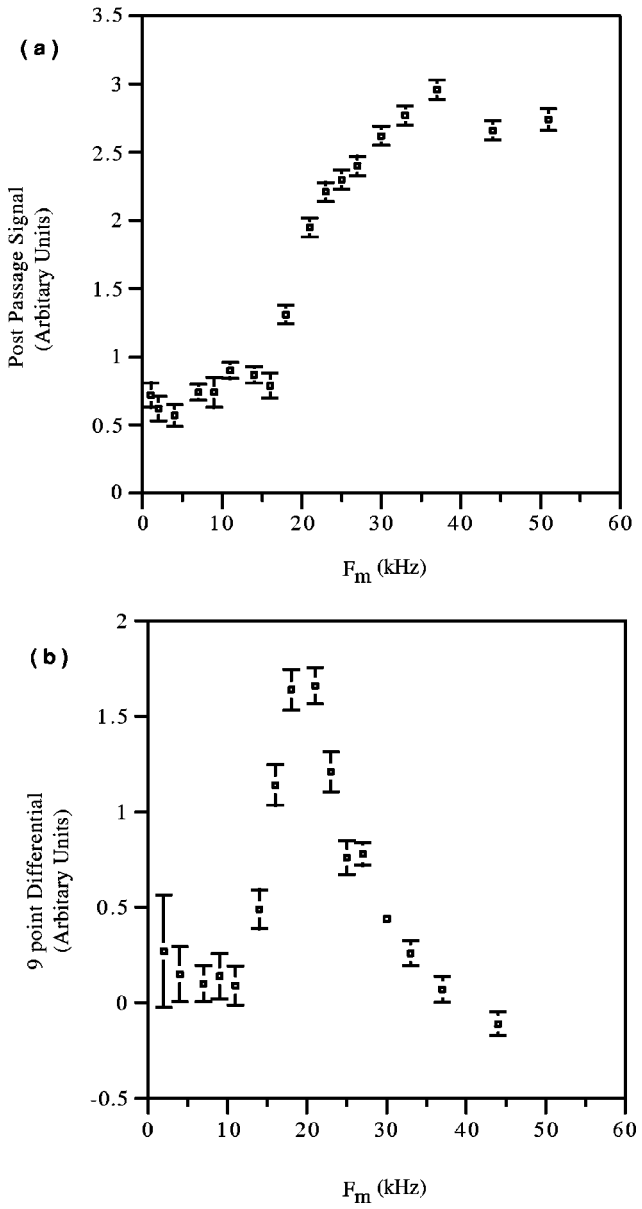

FIG. 4. Beta-detected MAPON on the ^{59}FeFe single crystal with 0.3 T applied along $\langle 111 \rangle$. (a) Shows the post passage change in anisotropy for sweep down experiments of 0.5-s duration, covering a 300-kHz range centered at 57.4 MHz. (b) The differential of (a) providing a mode value of $P/h = +20.2(5)$ kHz.

meanwhile, a theoretical estimate is required. Unfortunately, the two lowest $3/2^-$ states in ^{57}Fe and ^{59}Fe have quadrupole moments of the opposite sign (see Table I below and Ref. 23) which means that small changes in the shell-model interaction strongly affect the theoretical predictions of moments for these states. Even large-basis calculations have to be 'tuned' to reproduce the experimental magnetic moment of the $3/2_1^-$ state in ^{57}Fe.[23]

In view of this difficulty, and the fact that ^{59}Fe has an additional two valence nucleons which make large-basis shell-model calculations for it even more challenging than for ^{57}Fe, we have not attempted large-basis shell-model calculations. Instead we use a theoretical estimate based on the particle-rotor model. However, to justify this approach and provide an indication of the theoretical uncertainty in the adopted quadrupole moment, some limited-basis shell-model calculations were performed for the isotopes ^{56,57,58,59,60}Fe, using the interactions and effective charges ($\delta e_p = \delta e_n = 1.0$) of Vennick *et al.*[25] These calculations are compared with experiment in Table I. It was noted about 20 years ago that collective rotational structures appear in these nuclei and that they can be described microscopically through shell-model calculations.[26,27] The shell-model results for the even isotopes in Table I are in quite good agreement with experiment, but the predicted quadrupole moment for ^{59}Fe, $+0.235$ b, should be considered an upper limit since the calculations overestimate the transition rates in ^{60}Fe.

TABLE I. Shell-model calculations of $B(E2)$ $[e^2\ b^2]$ and Q $[b]$ values in the Fe isotopes with interactions and effective charges from Ref. 25.

Nuclide	Quantity	Experiment [a]	Shell model
^{56}Fe	$B(E2;2\rightarrow 0)$	0.0214(9)	0.0202
	$B(E2;4\rightarrow 2)$	0.0305(64)	0.0247
	$Q(2^+)$	$-0.23(3)$	-0.285
^{57}Fe	$Q(3/2_1^-)$	0.15(2), [b] 0.16(1) [c]	$+0.134$
	$Q(3/2_2^-)$		-0.139
^{58}Fe	$B(E2;2\rightarrow 0)$	0.0247(7)	0.0265
	$B(E2;4\rightarrow 2)$	0.0720(213)	0.0348
	$Q(2^+)$	$-0.27(5)$	-0.305
^{59}Fe	$Q(3/2_1^-)$		$+0.235$
	$Q(3/2_2^-)$		-0.221
^{60}Fe	$B(E2;2\rightarrow 0)$	0.0180(42)	0.0305
	$B(E2;4\rightarrow 2)$	0.0180(55)	0.0408
	$Q(2^+)$		-0.349

[a]Unless otherwise noted, experimental values are from Ref. 41.
[b]Reference 23
[c]Reference 24

Given that the states of interest in ^{59}Fe and its neighbors can be assigned a rotor-plus-particle nature, the particle-rotor model would appear to give a more reliable estimate of the ground-state quadrupole moment in ^{59}Fe than the limited-basis shell-model calculations performed to date. Beginning with the strong-coupling limit of the particle-rotor model, in which K is a good quantum number, we have

$$Q = Q_0[3K^2 - I(I+1)]/[(I+1)(2I+3)], \tag{1}$$

and

$$B(E2;0^+ \rightarrow 2^+) = (5/16\pi)e^2 Q_0^2, \tag{2}$$

where Q_0 is the intrinsic quadrupole moment. Note that in terms of the particle-rotor model the lowest two $3/2^-$ states in ^{57}Fe and ^{59}Fe are associated with two different rotational bands, the lowest with a $K = 3/2$ band, and the next with a $K = 1/2$ band. As such, these two states have quadrupole moments that are approximately equal in magnitude, but opposite in sign, as is indeed obtained in the shell-model calcula-

TABLE II. Intrinsic quadrupole moments in Fe isotopes.

Nuclide	E_x (keV)	I^π	Quantity [a]	Value [a]	Q_0 (b)
^{56}Fe	847	2^+	$B(E2;0\rightarrow 2)$	0.098(4)	0.992(20)
			$Q(2^+)$	$-0.225(28)$	$+0.79(10)$
^{57}Fe	14	$3/2^-$	$Q(3/2^-)$	$+0.15(2)$, [b] $+0.16(1)$ [c]	0.80(4)
					1.07(2) [d]
^{58}Fe	811	2^+	$B(E2;0\rightarrow 2)$	0.120(4)	1.098(18)
			$Q(2^+)$	$-0.27(5)$	$+0.95(18)$
^{59}Fe	0	$3/2^-$			1.06(4) [d]
^{60}Fe	824	2^+	$B(E2;0\rightarrow 2)$	0.093(18)	0.97(9)

[a] $B(E2)$ in $e^2\,b^2$ from Ref. 30; Q in b from Ref. 29, unless otherwise noted.
[b] Reference 23
[c] Reference 24
[d] Interpolated from neighboring $Q_0(2^+)$; see text.

tions shown in Table I as well as in the results for ^{57}Fe reported by Martínez-Pinedo *et al.*[23]

In Table II the Q_0 values obtained from experimental $B(E2)$ and quadrupole moment data for nuclei near ^{59}Fe, assuming the states have pure K, are compared. This is a good approximation for the even-A isotopes, but may not be so good for the odd-A cases. Values of Q_0 for ^{57}Fe and ^{59}Fe were also estimated by taking a three-point parabolic interpolation of the data for the even Fe isotopes, yielding $Q_0(^{57}\mathrm{Fe}) = 1.07 \pm 0.02$ b and $Q_0(^{59}\mathrm{Fe}) = 1.06 \pm 0.04$ b.

It is seen from Table II that there is reasonable consistency between the intrinsic quadrupole moments extracted from the $B(E2)$ values and the spectroscopic quadrupole moments in the even Fe isotopes. In the strong-coupling limit (pure K), the interpolated Q_0 values imply that $Q(3/2_1^-) \simeq +0.21(1)$ for both ^{57}Fe and ^{59}Fe, which clearly overestimates the quadrupole moment of ^{57}Fe.[23,24] In terms of the particle-rotor model, the quadrupole moment can be reduced by Coriolis mixing between states with $K = 3/2$ and $K = 1/2$. If this mixing is the same for ^{57}Fe and ^{59}Fe, then $Q(^{59}\mathrm{Fe}) \approx Q(^{57}\mathrm{Fe}) = 0.16$ b. These estimates are used to set upper and lower limits on the theoretical value adopted below, from particle-rotor model calculations that mix the $3/2^-$ states through Coriolis interactions.

Particle-rotor model calculations were performed for ^{59}Fe assuming an axially deformed core. The approach taken was to fix as many parameters as possible to standard values,[28] and use the very precisely measured magnetic moment of the ground state[15] as a further constraint. The quadrupole deformation parameter $\epsilon_2 = 0.2$ ($\epsilon_4 = 0$) was fixed from the interpolated Q_0 value in Table II. Similarly, the inertial parameter $E_{2^+} = 0.8$ MeV was chosen to be near $E(2^+)$ in ^{58}Fe and ^{60}Fe. Standard values of the Nilsson model parameters κ and μ were used.[28] The standard pairing force strengths for nuclei in this region were also used[28]. The magnetic moment was evaluated for $g_R = Z/A = 0.45$, which is very close to the experimental g factor for ^{58}Fe, $g = 0.46 \pm 0.13$,[29] and the spin g factor of the odd-nucleon was quenched to 0.7 times that of the bare neutron.

Since the deformation can be set by reference to the measured quadrupole moments in the even neighbors, in principle, the only model parameter that cannot be set to a standard value at the outset is the factor by which the Coriolis interactions must be attenuated from the Nilsson model values. The dependence of $Q(3/2^-)$ and $\mu(3/2^-)$ on the Coriolis attenuation factor is shown in Fig. 5. The particle-rotor

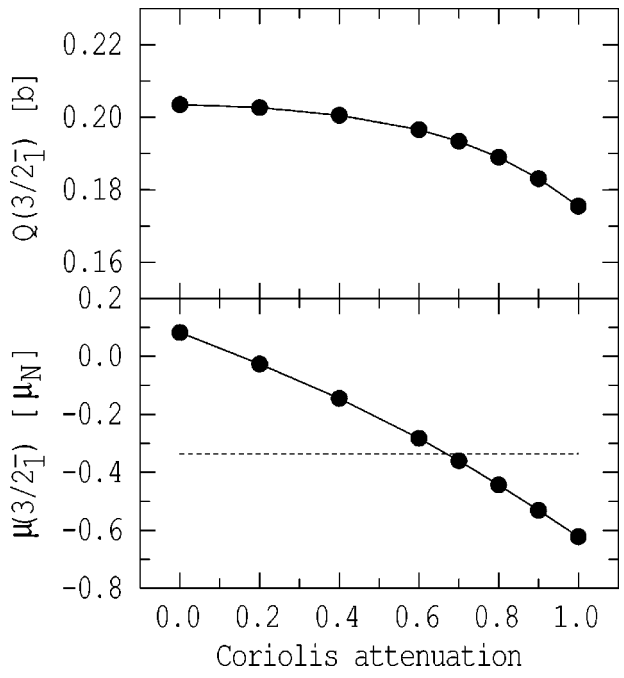

FIG. 5. Particle-rotor calculations of the quadrupole moment Q and the magnetic dipole moment μ for the ground state of ^{59}Fe as a function of the Coriolis interaction strength. The dotted line represents the experimental value of the magnetic moment (Ref. 15).

model can explain the measured ground-state magnetic moment of ^{59}Fe if the Coriolis interactions are attenuated to $\sim$70% of the Nilsson model values, which is typical of many cases.[28] The calculated quadrupole moment is then $Q(3/2_1^-) = +0.19$ b.

A similar calculation for ^{57}Fe gives $Q(3/2_1^-) = 0.16$ b, in excellent agreement with the recent recommended experimental values.[24,23] However, the magnetic moment is not well reproduced. We did not attempt to fine tune the calculation for ^{57}Fe because the magnetic moments are very sensitive to both the deformation and the strength of the Coriolis interactions, whereas the quadrupole moments are sensitive mainly to the deformation. As they stand, the calculations give consistent quadrupole moments for the lowest $3/2^-$ states in ^{57}Fe and ^{59}Fe with a reasonable parameter set that also gives a good description of the ground-state magnetic moment and the level scheme of ^{59}Fe. We adopt $Q(3/2^-) = +0.19 \pm 0.03$ b for ^{59}Fe, where the uncertainty is assigned based on uncertainties in the particle-rotor calculation and the extreme theoretical values encountered in the simple model estimates above.

V. DISCUSSION

The above MAPON results show that an EQI exists at the nucleus of isoelectronic ^{59}Fe in the cubic iron lattice that is just as significant as that observed for similar size $3d$ impurity probes when they are substitutional in an iron lattice. Precise quantitative efg comparisons are hampered by the lack of an accurate experimentally determined value for the ^{59}Fe nuclear quadrupole moment. However, as a result of the theoretical modeling presented in the previous section, the value of $Q(^{59}\mathrm{Fe},3/2^-) = +0.19(3)$ b is adopted to allow further progress. For $\langle 100\rangle$ and $\langle 111\rangle$, respectively, using $P/h = 3eQV_{ZZ}/4I(2I-1)h = +19.4(5)$ kHz $[+20.2(5)$ kHz] and $I = 3/2$ leads to $V_{ZZ}(^{59}\mathrm{FeFe}) = +1.7(3)\times 10^{19}$ V m^{-2} ($+1.8(3)\times 10^{19}$ V m^{-2}). It is interesting to compare these efg values with those derived from the pioneering work on pure iron using MES. Assuming the EQI sign should be as determined by our work, the rolled foil result at 4.2 K of Spijkerman *et al.* can be interpreted as $P/h = +2.2(18)$ μm s^{-1} $= +26(21)$ kHz. (Since a direct EQI sign measurement is not possible via MES at 4.2 K, caution must be exercised in making such an assumption. A strained polycrystalline foil could, in principle, show a nonintrinsic EQI value, even of opposite sign.[31]) Assuming that the measured Mössbauer shift corresponds to a principal EQI parallel to the $M1$ direction and using the $Q(^{57}\mathrm{Fe},3/2^-)$ value from Ref. 24, an efg at the Fe site of $V_{ZZ}(^{57}\mathrm{FeFe}) = +2.7(22)\times 10^{19}$ V m^{-2} is obtained. In a subsequent paper, Mercader and Cranshaw[10] were extremely critical of this result because of concerns over the issue of strain in the rolled Fe foil absorber. They also report EQI's of around 2(1) μm s^{-1} from their own MES studies but demonstrate changes in this quantity of similar magnitudes due to deliberately applied strains. A further tentative finding of Ref. 10 was a 50% increase in EQI between $\langle 100\rangle$ and $\langle 111\rangle$ directions for an Fe crystal plated with ^{57}Fe, which failed to reproduce at the time, is shown to be erroneous by the current MAPON study with the EQI in single-crystal Fe almost isotropic between the $\langle 100\rangle$ and $\langle 111\rangle$ directions. In summary, the early MES studies of EQI's in pure iron have been shown to have been indicative of the correct result by comparison with the superior resolution of MAPON. However, such measurements are right at the limit of resolution of the MES technique and perhaps, more critically, the need for high quality single crystals in such EQI measurements is incompatible with the technical requirements for a Mössbauer absorber.

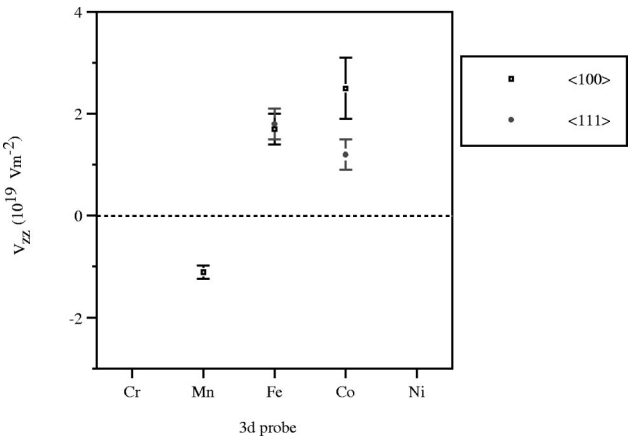

FIG. 6. Values of the electric field gradient (efg), derived from MAPON results, for three $3d$ probes in single-crystal bcc iron hosts.

The more important comparisons to be made with these FeFe efg results are with $3d$ impurities, nearby in the periodic table, placed in the iron host also obtained with MAPON. The FeFe results allow the first steps towards establishing the efg systematics for $3d$ probes in the cubic $3d$ ferromagnetic hosts. The efg at the Fe nucleus in Fe has the same sign and similar magnitude to that for Co. However, Co has a large anisotropy as a function of crystal direction, $V_{ZZ}(^{60}\mathrm{CoFe}) = +2.5(6)\times 10^{19}$ V m^{-2} $[+1.2(3)\times 10^{19}$ V m$^{-2}]$ for $\langle 100\rangle$ and $\langle 111\rangle$, respectively.[17,32] In contrast, a sign change and slightly smaller magnitude is observed for the S state Mn probe,[33] $V_{ZZ}(^{54}\mathrm{MnFe}\langle 100\rangle) = -1.11(13)\times 10^{19}$ V m^{-2}. It should be noted that all efg's at $3d$ probes in single-crystal Fe and Ni,[16] including Mn probes, are considerably larger in magnitude then those associated with distant point defects in[34] undeformed nonmagnetic elemental cubic hosts such as copper[35] or silver. With MAPON resolution, it was reported previously[36] that the efg at the ^{110m}Ag probe, even in highly faulted polycrystalline silver, is an order of magnitude smaller than the efg's at $3d$ probes in the cubic ferromagnets. The emerging trend for efg's in bcc iron for probes near in size and mass to the host is illustrated in Fig. 6. The most obvious question posed by this limited data set is the origin of the sign reversal for Mn in Fe. It should be noted that the negative efg for ^{54}MnFe is consistent with the known broader trends for efg's at $3d$ probes in the cubic ferromagnetic hosts. For example, there is an observed change of efg sign for a given $3d$ probe from bcc iron to fcc Ni. For Co in Fe the efg is positive while for Co in Ni it is negative.[16] The sign change is also seen for ^{54}Mn, in reverse order, with $V_{ZZ}(^{54}\mathrm{MnNi})$ being positive.[37]

This complementary sign change for the Mn probe compared to Fe and Co probes appears general, and is of significance. However, it is unwise, at this point to conclude that these differences are solely the result of the *S* state nature of the Mn impurity in Fe. It could be argued that the trend displayed in Fig. 6 is qualitatively similar to the eyeball $M1$ plots for $3d$ impurity hyperfine field systematics in Fe.[2] However, in this latter case the baseline is not near zero but has a substantial offset due to a transferred magnetic hyperfine field, via conduction electron polarization, from the host ferromagnet.

The observation that the efg distribution for the isoelectronic probe in Fe is around twice as broad with magnetization along the $\langle 100 \rangle$ compared with the $\langle 111 \rangle$ is interesting. Although it mirrors similar results for $5d$ probes in Fe,[21] clearly it strongly suggests that the underlying mechanism, in both cases, is intrinsic to the Fe host. Other comparisons between the efg's in the cubic ferromagnets of $3d$ and $5d$ impurity probes are also instructive. With the advent of the MAPON technique it became immediately apparent that efg's in the nominally cubic ferromagnets are in general anisotropic as a function of crystal direction. Anisotropy was indeed seen, for the $3d$ probe Co, in the earliest MAPON studies.[42] For heavier mass $5d$ probes, even though the efg's are about an order of magnitude larger, it again required MAPON resolution to show efg anisotropy.[38] In both the $3d$ and $5d$ cases the amount of anisotropy depends on the particular probe. Anisotropy is large for Co and Ir and ranges down to close to negligible for Mn and Re. There are, however, also significant differences between the $3d$ and $5d$ cases. Unlike the $3d$ case discussed above, $5d$ impurities such as Ir do not exhibit opposite sign efg's in Fe (bcc) and Ni (fcc) hosts. This difference between $5d$ and $3d$ probes as well as other considerations like the extremely small efg's found for the intermediate $4d$ probe set, led to the earlier proposal that there are two competing mechanisms to be considered, one which is dominant in the $3d$, the other for the $5d$.[16] Historically, theoretical treatments, for example Ref. 8, were based on modeling early apparently isotropic $5d$ data and used spin-orbit coupling to induce orbital angular momentum at the impurity site. This approach still appears optimal for the $5d$ case assuming that the addition of explicit $5d$ band structure of the impurity in question can predict the required efg anisotropy. For $3d$ probes an alternative approach is possible. Inherent unquenched orbital angular momentum on the probe, originating from the free-atom configuration, sensitive to crystal-field effects, could provide the primary contribution to the efg. From this proposal it follows that for isoelectronic probe nuclei in pure Fe, Ni, and fcc Co, efg's similar to those obtained for nearby (non-*S*-state) impurity probes placed in comparable hosts are expected. The current results for Fe support this premise. Likewise, for Co probes in the fcc hosts Co and Ni, very similar efg results are obtained for the elemental case CoCo, albeit in a polycrystalline host[39] $[V_{ZZ}(^{60}\mathrm{CoCo}) = -3.5(5) \times 10^{19}\ \mathrm{V\,m^{-2}}]$, and in the case where Co is an impurity in single-crystal Ni[16] $[V_{ZZ}(^{60}\mathrm{CoNi}\langle 111 \rangle) = -3.6(3) \times 10^{19}\ \mathrm{V\,m^{-2}}]$. From the established systematics it can be predicted that Mn will experience a positive efg in fcc Co, and Ni impurities will experience a positive efg in bcc Fe. The first of these predictions has now been verified experimentally.[40]

Clearly there is scope for further work to fully establish the efg systematics at $3d$ probes in all three $3d$ cubic ferromagnets. The successful realization of beta-detected MAPON implies that it is experimentally feasible to greatly expand the range of the nd probe efg data set in ferromagnets. Beta detection can circumvent the lack of suitable gamma-emitting LTNO probes in a number of instances and potentially allows the use of more sensitive probes in others. For example, in the $3d$ case at hand, ^{57}Ni has yielded beta-detected NMRON,[15] and is a potential Ni probe candidate. Ni like Fe is an element without a suitable gamma-emitting NMRON probe. Additionally ^{46}Sc, ^{48}V, ^{48}Cr, and ^{67}Cu are all potential $3d$ probes for such studies.

ACKNOWLEDGMENTS

W.D.H. would like to acknowledge with thanks the Australian Academy of Science and the Japan Society for the Promotion of Science for an award under the AAS-JSPS exchange program.

[1] K. S. Krane, Hyperfine Interact. **15/16**, 1069 (1983).
[2] N. J. Stone, in *Low-Temperature Nuclear Orientation*, edited by N. Stone and H. Postma (North-Holland, Amsterdam, 1986), Chap. 8, p. 351.
[3] M. Akai, H. Akai, and J. Kanamori, J. Phys. Soc. Jpn. **54**, 4246 (1985).
[4] H. Akai, M. Akai, S. Blügel, B. Drittler, H. Ebert, K. Terakura, R. Zeller, and P. H. Dederichs, Prog. Theor. Phys. Suppl. **101**, 11 (1990).
[5] H. Akai and T. Kotani, Hyperfine Interact. **120/121**, 3 (1999).
[6] H. Akai, Hyperfine Interact. **43**, 255 (1988).
[7] M. Aiga and J. Itoh, J. Phys. Soc. Jpn. **37**, 967 (1974).
[8] G. A. Gehring and H. C. L. Williams, J. Phys. F: Met. Phys. **4**, 291 (1974).
[9] C. Demangeat, J. Phys. F: Met. Phys. **5**, 169 (1975).
[10] R. C. Mercader and T. E. Cranshaw, J. Phys. F: Met. Phys. **5**, L124 (1975).
[11] P. T. Callaghan, P. J. Back, and D. H. Chaplin, Phys. Rev. B **37**, 4900 (1988).
[12] J. J. Spijkerman, J. C. Travis, D. N. Pipkorn, and C. E. Violet, Phys. Rev. Lett. **26**, 323 (1971).
[13] R. Angers and F. Claisse, Can. Metall. Q. **7**, 73 (1968).
[14] D. H. Chaplin and W. D. Hutchison, Hyperfine Interact. **75**, 209 (1992).
[15] T. Ohtsubo, D. J. Cho, Y. Yanagihashi, S. Ohya, and S. Muto, Phys. Rev. C **54**, 554 (1996).
[16] W. D. Hutchison, N. Yazidjoglou, and D. H. Chaplin, Aust. J. Phys. **51**, 295 (1998).
[17] P. J. Back, D. H. Chaplin, and P. T. Callaghan, Phys. Rev. B **37**, 4911 (1988).

[18] T. Ohtsubo (private communication).
[19] P. C. Riedi, J. Phys. F: Met. Phys. **5**, 186 (1975).
[20] P. T. Callaghan, P. D. Johnston, and N. J. Stone, J. Phys. C **7**, 3161 (1974).
[21] G. Seewald, E. Hagn, E. Zech, R. Kleyna, M. Voß , D. Forkel-Wirth, A. Burchard, and ISOLDE Collaboration, Phys. Rev. Lett. **82**, 1024 (1999).
[22] P. C. Sood, Phys. Rev. **179**, 1100 (1969).
[23] G. Martínez-Pinedo, P. Schwerdtfeger, E. Caurier, K. Langanke, W. Nazarewicz, and T. Söhnel, Phys. Rev. Lett. **87**, 062701 (2001).
[24] P. Dufek, P. Blaha, and K. Schwarz, Phys. Rev. Lett. **75**, 3545 (1995).
[25] R. Vennick, J. Kopecky, P. M. Endt, and P. W. M. Glaudemans, Nucl. Phys. A **344**, 421 (1980).
[26] J. B. McGrory and S. Raman, Phys. Rev. C **20**, 830 (1979).
[27] R. B. M. Mooy and P. W. M. Glaudemans, Z. Phys. A **312**, 59 (1983).
[28] P. B. Semmes and I. Ragnarsson (unpublished), distributed at the Hands-on Nuclear Theory Workshop, Oak Ridge, 5–16 August, 1991.
[29] P. Raghavan, At. Data Nucl. Data Tables **42**, 189 (1989).
[30] S. Raman, C. H. Malarkey, W. T. Milner, C. W. Nester, Jr., and P. H. Stelson, At. Data Nucl. Data Tables **36**, 1 (1987).
[31] H. R. Foster, D. H. Chaplin, P. Lynam, D. E. Swan, and G. V. H. Wilson, Hyperfine Interact. **10**, 1143 (1981).
[32] P. J. Back, Hyperfine Interact. **43**, 211 (1988).
[33] N. Yazidjoglou, W. D. Hutchison, and G. A. Stewart, J. Phys.: Condens. Matter **6**, 7109 (1994).
[34] O. Kanert, D. Kotzur, and M. Mehring, Phys. Status Solidi **36**, 291 (1969).
[35] O. Kanert and M. Mehring, in *NMR—Basic Principles and Progress*, edited by P. Diehl, E. Fluck, and R. Kosfeld (North-Holland, New York, 1971), Vol. 3, p. 74.
[36] W. D. Hutchison, N. Yazidjoglou, and D. H. Chaplin, Hyperfine Interact. **75**, 253 (1992).
[37] D. H. Chaplin, W. D. Hutchison, M. P. Kopp, and N. Yazidjoglou, Hyperfine Interact. **43**, 241 (1988).
[38] G. Seewald, E. Hagn, E. Zech, D. Forkel-Wirth, A. Burchard, and The ISOLDE Collaboration, Phys. Rev. Lett. **78**, 1795 (1997).
[39] W. D. Hutchison, A. V. J. Edge, N. Yazidjoglou, and D. H. Chaplin, Phys. Rev. Lett. **67**, 3436 (1991).
[40] W. D. Hutchison, A. V. J. Edge, and D. H. Chaplin, in Proceedings of the 12th International Conference on Hyperfine Interactions, Park City, Utah, 2001 [Hyperfine Interact. (to be published)].
[41] H. Junde, Nucl. Data Sheets **86**, 315 (1999); M. R. Bhat, *ibid.* **85**, 415 (1998); **80**, 789 (1997); C. M. Baglin, *ibid.* **69**, 733 (1993); M. M. King, *ibid.* **69**, 1 (1993).
[42] P. J. Back, Hyperfine Interact. **43**, 211 (1988).